# Chapter 6

# Preparation and characterization of spray dried lansoprazole enteric microparticles

### 6.1. Lansoprazole- Drug Profile

Lansoprazole (LSP), a BCS class II compound belongs to the category of compounds called proton pump inhibitors (PPIs). They have been explicitly employed in the treatment of gastroesophageal reflux disease, erosive esophagitis, heartburn, Zollinger-Ellison syndrome and long term treatment of pathological hypersecretory conditions [1-3].

**General Characteristics:** [4-8]

- **Molecular Formula:** $C_{16}H_{14}F_3N_3O_2S$
- **IUPAC Name:** 2-[[[3-methyl-4-(2,2,2-trifluoroethoxy)-2-pyridyl] methyl] sulfinyl] benzimidazole
- **Structure:**

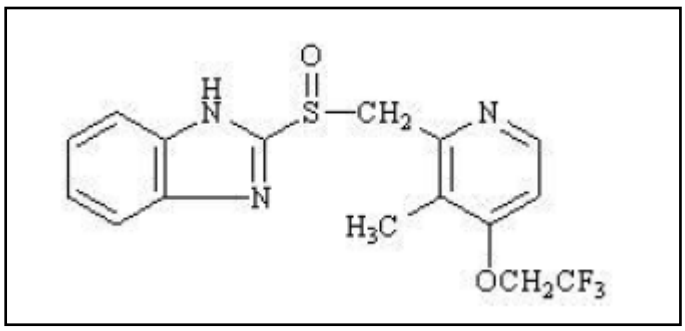

- **Molecular weight:** 369.363
- **Appearance and Color:** white to brownish white crystalline powder.
- **Odor:** Odorless.
- **Solubility:** Soluble in methanol and chloroform but very slightly soluble in water.
- **Melting point:** 178 to 182$^{o}$C with decomposition.
- **Dissociation constants:** 2.34±0.37, 3.53±0.37 and 8.48±0.30.
- **Octanol/Water Partition Coefficient**: log Kow = 2.39 ± 0.78.
- **Dose**: 15 mg and 30 mg.
- **Stability**: Lansoprazole is unstable in acidic media.

**Mechanism of action**

PPIs gets converted into active sulfenamide metabolite by the acidic environment of parietal cells which further reacts with cysteins of enzyme H+/K+ ATPase. This causes inactivation of sulphydryl group of the proton pump thereby reducing the hydrogen ion concentration. This conversion of LSP into active form should occur

inside the gastric cells, thus it should be absorbed in intact form from the intestinal tract [1, 3, 9].

**Pharmacokinetics**

Lansoprazole is rapidly absorbed after oral administration with peak plasma concentration achieving around 1.7 hr. The absolute bioavailability is greater than 80% in fasted state. Absorption decreases if taken 30 minutes after meal as compare to fasting condition. It does not accumulate in the body and hence, its pharmacokinetics is not altered upon multiple dosing. Lansoprazole is 97% bound to the plasma proteins. Lansoprazole is metabolized by liver and it undergoes minimal first pass metabolism. The two main metabolites are the hydroxylated sulfinyl and sulfone derivatives of lansoprazole. The two main metabolites have very little or no antisecretory activity. Studies indicate predominantly biliary excretion of the metabolites [6, 8, 10].

**Indications and Usage**

Gastroesophageal reflux disease, erosive esophagitis, heartburn, Zollinger-Ellison syndrome , peptic ulcer, etc. [1-3, 8, 10].

**Contraindications**

Lansoprazole is contraindicated in patients with known hypersensitivity to the drug [8].

**Drug Interactions**

Lansoprazole interferes with the absorption of drugs where gastric pH is prerequisite for oral bioavailability like atazanavir, digoxin, ketoconazole, etc. [8]

**Adverse Effects**

The frequent side effects observed are with gastrointestinal which incude nausea, diarrhea and abdominal pain. Other side effects observed are headache, pharyngitis, dermatological, endocrinal, cardiovascular, lymphatic, etc. which are less frequently observed [10].

## 6.2. Analytical Methods

### 6.2.1. Determination of LSP at 292nm by UV – spectrophotometric method

This method was used to determine entrapment efficiency in the preliminary trial batches.

#### 6.2.1.1. Preparation of standard stock solutions of LSP

LSP (100 mg) was dissolved in 60 ml of 0.1N NaOH and adjusting the final volume upto 100 ml by phosphate buffer pH 6.6 to prepare stock solution of 1000 µg/ml. An aliquot of 10 ml was accurately taken out with graduated calibrated pipette and further diluted upto 100 ml with 0.01N NaOH to obtain working standard solution of 100 µg/ml.

#### 6.2.1.2. Preparation of calibration curve of LSP

Varying concentrations of LSP (5-30 µg/ml) were prepared with appropriate dilutions of stock solution with 0.01N NaOH as diluent. The absorbance was measured at 292 nm using UV spectrophotometer with 1 cm quartz cuvettes and calibration curve was plotted against concentration (µg/ml).

Accuracy and precision were carried out as per ICH guidelines [11]. For accuracy measurements were taken in triplicate and for precision six determinants were measured. The results of accuracy and precision are depicted in Table 1 and Table 2 respectively No interference of excipients was found at specified detection wavelength.

The reference spectrum of LSP is depicted in Fig. 1. The calibration curve of LSP, regression analysis equation and correlation coefficient is depicted in Fig. 2 respectively.

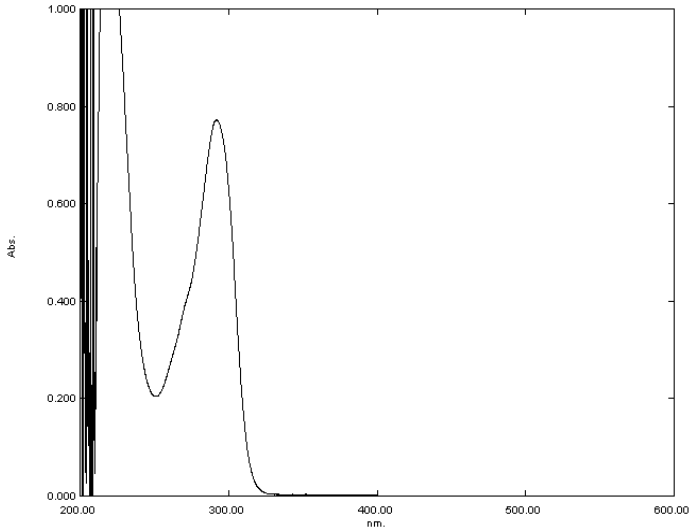


**Fig. 1: Reference spectra of LSP in at 292 nm using UV spectrophotometry.**

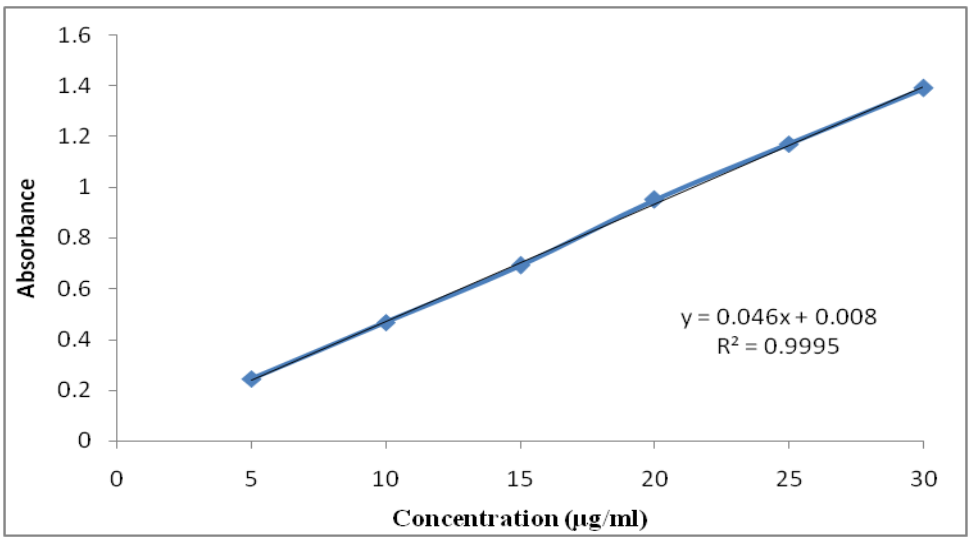


**Fig. 2: Calibration curve of LSP at 292 nm using UV spectrophotometry.**

**% Recovery:**

**Table 1: % Recovery for LSP**

| Amount of Sample Taken Equivalent to (mg) | Amount of Sample Spiked (mg) | Amount of Spiked Sample Recovered | % Recovery |
|---|---|---|---|
| 10 | 6 | 5.97±0.06 | 99.50 |
| 10 | 10 | 10.11±0.08 | 101.10 |
| 10 | 14 | 13.91±0.15 | 99.36 |

Data are represented as Mean± SD (n=3)

**Precision:**

**Table 2: Precision for LSP**

| | % Relative Standard Deviation |
|---|---|
| Repeatability | 0.98 |
| Intraday | 1.51 |
| Interday | 1.85 |

### 6.2.2. Determination of LSP in phosphate buffer pH 7.4 at 292nm by UV – spectrophotometric method

This method was used for estimation of LSP during dissolution in the preliminary trial batches.

#### 6.2.2.1. Preparation of standard stock solutions of LSP

LSP (100 mg) was dissolved in 60 ml of 0.1N NaOH and adjusting the final volume upto 100 ml by phosphate buffer pH 6.6 to prepare stock solution of 1000 µg/ml. An aliquot of 10 ml was accurately taken out with graduated calibrated pipette and further diluted upto 100 ml with pH 7.4 phosphate buffer to obtain working standard solution of 100 µg/ml.

#### 6.2.2.2. Preparation of calibration curve of LSP

Varying concentrations of LSP (5-30 µg/ml) were prepared with appropriate dilutions of stock solution with pH 7.4 phosphate buffer. The absorbance was measured at 292 nm using UV spectrophotometer with 1 cm quartz cuvettes and calibration curve was plotted against concentration (µg/ml).

Accuracy and precision were carried out as per ICH guidelines [11]. For accuracy measurements were taken in triplicate and for precision six determinants were measured. The results of accuracy and precision are depicted in Table 3 and Table 4 respectively. No interference of excipients was found at specified detection wavelength.

The reference spectrum of LSP in phosphate buffer pH 7.4 is depicted in Fig. 3. The calibration curve of LSP in phosphate buffer pH 7.4, regression analysis equation and correlation coefficient is depicted in Fig. 4 respectively.

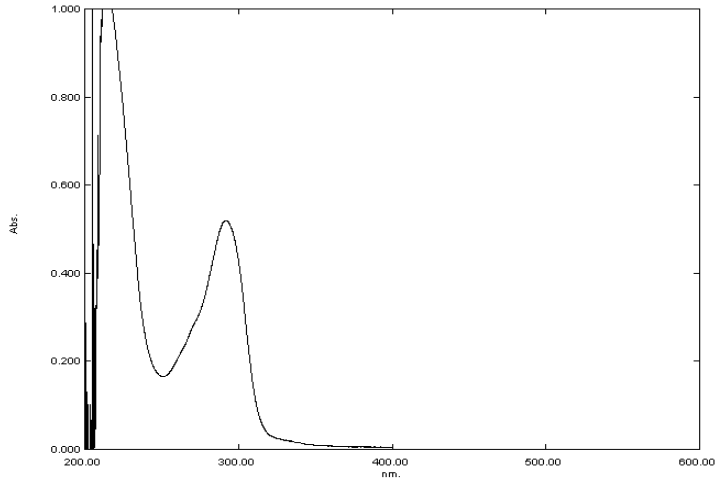


**Fig. 3: Reference spectra of LSP in phosphate buffer pH 7.4 at 292 nm.**

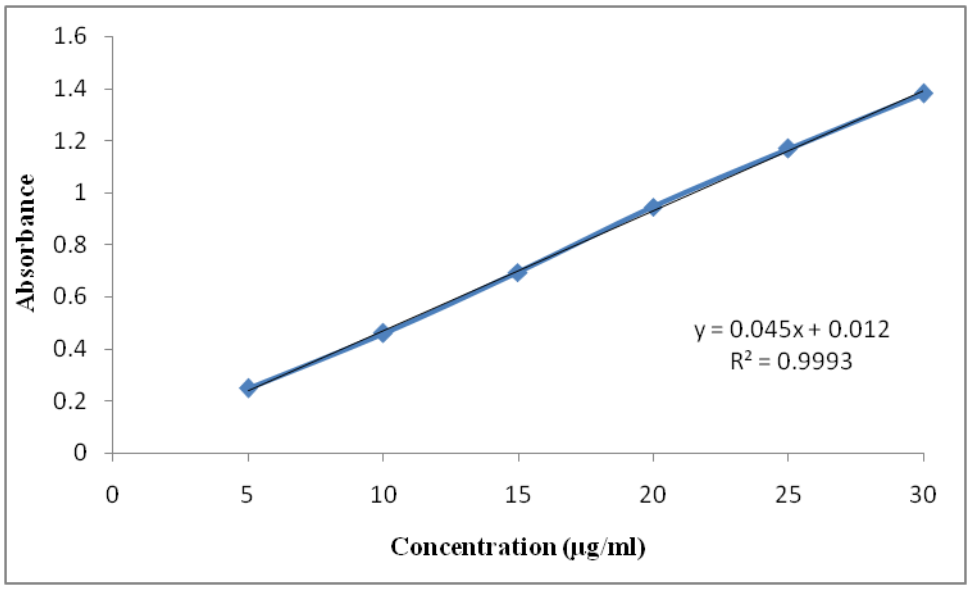


**Fig. 4: Calibration curve of LSP in phosphate buffer pH 7.4 at 292 nm**

**% Recovery:**

**Table 3: % Recovery for LSP**

| Amount of Sample Taken Equivalent to (mg) | Amount of Sample Spiked (mg) | Amount of Spiked Sample Recovered | % Recovery |
|---|---|---|---|
| 10 | 6 | 6.05±0.05 | 100.83 |
| 10 | 10 | 9.93±0.08 | 99.30 |
| 10 | 14 | 13.96±0.12 | 99.71 |

Data are represented as Mean± SD (n=3)

**Precision:**

**Table 4: Precision for LSP**

| | % Relative Standard Deviation |
|---|---|
| Repeatability | 0.80 |
| Intraday | 1.21 |
| Interday | 1.66 |

### 6.2.3. Determination of LSP by reverse phase high performance liquid chromatography method (RP-HPLC):

This method was used to determine entrapment efficiency and dissolution for final batches. Gastric resistance for all the batches was measured by this method.

#### 6.2.3.1. HPLC instrumentation and conditions

Chromatography was performed on Shimadzu (Shimadzu Corporation, Kyoto, Japan) chromatographic system equipped with Shimadzu LC-20AT pump and Shimadzu SPD-20AV UV detector. Samples were injected through a Rheodyne 7725 injector valve with fixed loop of 20 µL. The chromatographic separation was achieved using isocratic method as per below mentioned parameters (Table 5). The mobile phase was vacuum filtered through 0.22 µm nylon membrane filter followed by degassing in an ultrasonic bath prior to use. Data acquisition and integration was performed using Spinchrome software (Spincho Biotech, Vadodara).

**Table 5: HPLC parameters for estimation of LSP.**

| Parameter | Condition |
|---|---|
| Column | Phenomenax C18 (250 mm × 4.6 mm i.d., 5 µm particle size) |
| Mobile Phase | Water:Acetonitrile:Triethylamine (45:55:1), pH 7 |
| Diluent | Water:Acetonitrile:Triethylamine (45:55:1), pH 10 |
| Flow rate | 1 ml/min |
| Detection wavelength | 285 nm |
| Injection volume | 20 µl |

### 6.2.3.2. Preparation of standard stock solutions of LSP

LSP (100 mg) was dissolved in 50 ml of diluent and volume was made up to 100 ml with diluent to obtain stock solution of 1000µg/ml. An aliquot of 10 ml was accurately taken out with graduated calibrated pipette and further diluted upto 100 ml with diluent to obtain working standard solution of 100 µg/ml.

### 6.2.3.3. Preparation of calibration curve of LSP

Varying concentrations of LSP (1-90 µg/ml) were prepared with appropriate dilutions of stock solution with diluent (Table 5). Calibration graph (Fig. 6) was constructed by plotting area versus concentration of LSP and the regression equation was calculated. The reference chromatogram of LSP is depicted in Fig.5 and calibration curve of LSP, regression analysis equation and correlation coefficient is depicted in Fig. 6. System suitability test was performed by injecting six consecutive samples of 30µg/ml during start of method validation. The parameters observed were retention time, tailing factor, theoretical plates and %relative standard deviation (%RSD) of area. The data are represented in Table 6. The accuracy and precision data are represented in Table 7 and Table 8 respectively.

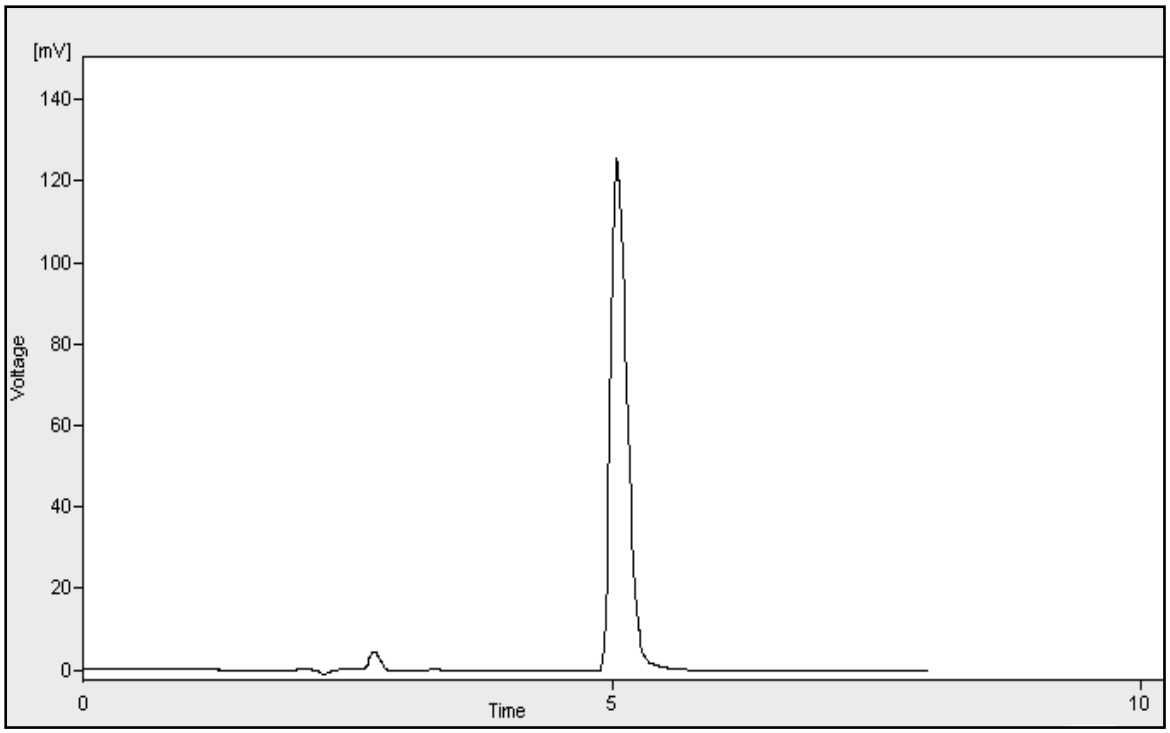


**Fig. 5: Reference chromatogram of LSP taken using HPLC method.**

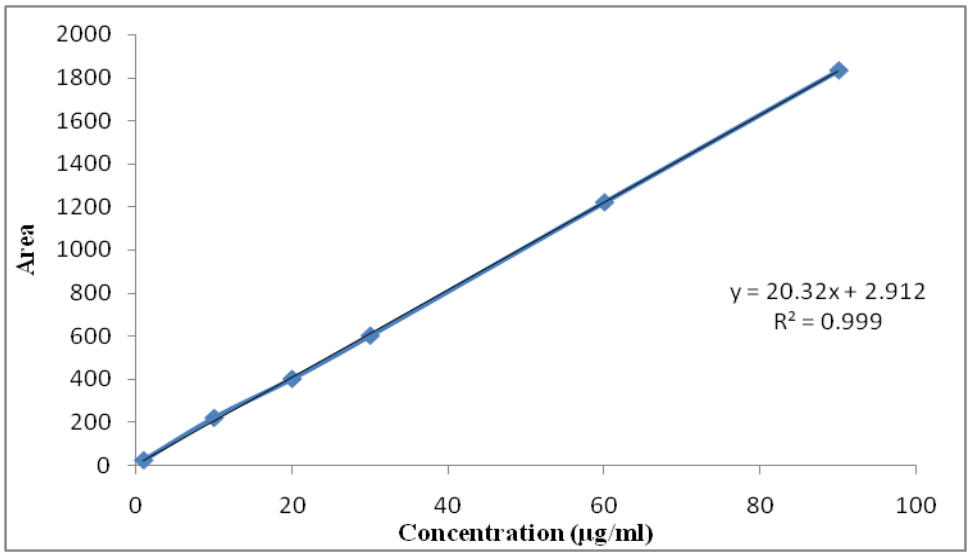


**Fig. 6: Calibration curve of LSP taken using HPLC method**

**System suitability parameters**

**Table 6: System suitability parameters for estimation of LSP**

| Parameters | Mean±SD |
|---|---|
| Retention time (min) | 5.03±0.03 |
| Asymmetry | 1.1±0.06 |
| Theoretical plate | 6995.65±33.32 |
| %RSD of area | 0.91 |

**% Recovery:**

**Table 7: % Recovery for LSP**

| Amount of Sample Taken Equivalent to (mg) | Amount of Sample Spiked (mg) | Amount of Spiked Sample Recovered | % Recovery |
|---|---|---|---|
| 20 | 12 | 12.11±0.11 | 100.92 |
| 20 | 20 | 19.95±0.15 | 99.75 |
| 20 | 28 | 27.92±0.18 | 99.71 |

Data are represented as Mean± SD (n=3)

**Precision:**

**Table 8: Precision for LSP**

| | % Relative Standard Deviation |
|---|---|
| Repeatability | 0.91 |
| Intraday | 1.33 |
| Interday | 1.81 |

## 6.3. Methods

### 6.3.1. Preparation of microparticles by spray drying

The spray drying operation was performed using a laboratory scale spray dryer (LU-227, Labultima, Mumbai, India). Firstly polymer was dispersed in half quantity of required water which was subsequently neutralized by addition of sodium hydroxide (NaOH) till pH 9 was obtained. pH 9 was selected as it was reported to be the most stable pH for LSP where its degradation is minimum [12]. To this neutralized solution of enteric polymer, finely grounded LSP (sifted through ASTM # 150) was slowly added and dispersed into it. Finally, the water was added to adjust the desired feed solution concentration.

### 6.3.2. Process parameter optimization

Spray drying has variegated parameters which need to be optimized to ascertain desired quality traits. The consequences of diverse process parameter on product attributes together with the range of their variation were studied. The following parameters were investigated; inlet air temperature, atomizing air pressure, feed solution concentration, feed solution spray rate and aspirator volume. Each parameter was varied at a time while keeping others constant, considering their relative impact on product attributes. The value selected for parameter investigated was carried forward in subsequent trials.

### 6.3.3. Evaluation of microparticles

#### 6.3.3.1. Entrapment efficiency

Initially, the microparticles were washed with acetonitrile to remove the free drug. Then the microparticles were dried in vacuum oven (Ohmkar Equipments, India) at

$30^0$ C for overnight. Subsequently, microparticles equivalent to 30 mg LSP were weighed and transferred to a 100 ml volumetric flask. The drug content was analyzed by developed UV-spectrophotometric and HPLC method as discussed in section 6.2.
To determine the entrapment efficiency, the following practical relationship was used
Entrapment efficiency = Weight of drug incorporated/ Weight of drug initially taken × 100

#### 6.3.3.2. *In vitro* gastric resistance

The gastric resistance study was evaluated using United States Pharmacopeia (USP) 29 type II apparatus (VDA 6-DR,Veego Instruments Corporation, Mumbai, India) using 500 ml of 0.1 N hydrochloric acid (HCl) at 75 rpm rotation speed and 37 ◦C±0.5 ◦C temperature for 60 minutes. Here, prior performing dissolution in 0.1N HCL, assay was carried out for microparticles. After 1 hr, sample was removed and assayed again. The difference in the assay was calculated as gastric resistance or the amount of drug degraded in acidic media. A validated HPLC method was used for drug content measurement as discussed in section 6.2.3.

#### 6.3.3.3. *In vitro* drug release study

Dissolution was carried out using USP 29 type II apparatus (VDA 6-DR, Veego Instruments Corporation, Mumbai, India) using 500 ml of 0.1 N hydrochloric acid (HCl) at 75 rpm rotation speed and 37 ◦C±0.5 ◦C temperature for 60 minutes as mentioned in USP [13] followed by buffer stage consisting of 900 ml phosphate buffer pH 7.4 for 60 minutes. Samples were removed from the dissolution media in different time intervals and during an equal volume of dissolution medium replaced at each sampling time to maintain constant media volume. Samples withdrawn were withdrawn were filtered through a 0.45 μm membrane filter and then analyzed for drug release by UV-spectrophotometric and HPLC method as described in above section 6.2.

#### 6.3.3.4. Gastric resistance and *in vitro* drug release in modified acid stage medium pH 4.5

The enteric performance is usually carried out in acidic media at pH 1.2. However, it is reported that stomach pH for PPIs on multiple regiment is >4 and hence, enteric performance of various enteric polymer must be verified at higher pH or biorelavent

media better simulating the gastric environment have been suggested [14]. Thus, microparticles were investigated for gastric resistance in modified acidic media consisting of pH 4.5 acetate buffer followed by *in vitro* drug release in phosphate buffer pH 7.4 by same procedure as described for *in vitro* drug release.

**6.3.3.5. Particle size analysis**

The average particle diameter and size distribution of microparticles were determined by using Malvern (Mastersizer 2000, Malvern Instruments, UK) after its dispersion in iso-octane. An aliquot of the microparticle suspension was then added into the small volume recirculation unit and circulated at 3500 rpm. Each sample was measured in triplicate in the analysis.

**6.3.3.6. Scanning electron microscopy (SEM) study**

The purpose of the SEM study was to obtain topographical images of microparticles. SEM photographs were taken using a scanning electron microscope (JEOL JSM-5610LV, Japan) at the required magnification at room temperature after they were gold sputtered. The acceleration voltage used was 10 kV, with the secondary electron image as the detector.

**6.3.3.7. Differential scanning calorimetry (DSC) study**

DSC was of pure LSP, physical mixture of drug and Eudragit S-100, blank microparticles and drug loaded microparticles were crimped in a standard aluminum pan and heated from 40˚C to 300˚C at a heating rate of 5˚C/min under constant purging of dry nitrogen at 40 ml/min. DSC thermograms were obtained using an automatic thermal analyzer system (DSC-60, Shimadzu, Japan). Temperature calibration was performed using indium as the standard. An empty pan, sealed in the same way as the sample, was used as the reference.

**6.3.3.8. Fourier transform infra-red (FT-IR) spectroscopy study**

The FT-IR (Bruker, USA) spectra of the pure drug, physical mixture of drug and Eudragit S100, blank microparticles and drug loaded microparticles were investigated using potassium bromide (KBr) disk method. In brief procedure involved mixing of 2% (w/w) of the sample with respect to the KBr (S. D. Fine Chem Ltd., Mumbai, India). The mixture of drug and dry KBr was ground into an agate mortar and was

compressed into a KBr pellet under a hydraulic press at10,000 psi. Each KBr disk was scanned 16 times at 4 mm/s at a resolution of 2 $cm^{-1}$ over a wavenumber range of 400–4000 $cm^{-1}$. The characteristic peaks were recorded.

### 6.3.3.9. Powder X-Ray Diffraction Study

Powder X-ray diffraction (PXRD) patterns of the pure drug, physical mixture of drug and Eudragit S-100, blank microparticles and drug loaded microparticles were investigated using powder Xray diffractometer (Philips X'Pert, The Netherlands). An X-ray beam (Philips Cu target X-ray tube) was allowed to fall over the sample. As the slide moves at an angle of theta degree, a proportional detector detects diffracted X-rays at angle of 2θ° and subsequently XRD patterns were recorded. XRD patterns were recorded in the 2θ° range of 5 to 60.

### 6.3.4. Batch reproducibility, packaging and stability study

Three batches of the optimized formulation were prepared and evaluated under the identical conditions. Moreover, the optimized batch was subjected to short term stability testing according to the ICH guidelines [15]. Microparticles equivalent to 250 mg of LSP were filled in amber color glass vials which were further sealed. The desiccant silica bag was kept inside glass vial by adhering it to the inside part of teflon closure before sealing it. Alternatively, final capsule formulation kept in amber color bottle with dessicant silica beg was also charged on stability. The sealed vials/bottle were exposed to accelerated (40±2 ◦C/75±5% relative humidity) and long term (25±2 ◦C/60 ± 5% relative humidity) stability for three months. The samples were withdrawn periodically (0, 15, 30, 60 and 90 days) and evaluated for different parameters like visual appearance, powder characteristics, entrapment efficiency and *in vitro* drug release.

## 6.4. Results and Discussion

### 6.4.1. Preliminary trials for evaluation of type of enteric polymer and its level

**Table 9: Preliminary trials for evaluation of type of enteric polymer and its level.**

| Sr. No. | Batch No. | Ingredients | Drug : Polymer ratio | EE* | GR# |
|---|---|---|---|---|---|
| | | Preliminary trials | | | |
| 1 | B1 | HPMCAS LF | 1:3 | 30.55±2.3 | - |
| 2 | B2 | HPMCAS LF | 1:5 | 50.23±1.8 | 60.12±2.9 |
| 3 | B3 | HPMCAS HF | 1:3 | 32.95±1.9 | - |
| 4 | B4 | HPMCAS HF | 1:5 | 46.69±2.9 | 46.35±2.3 |
| 5 | B5 | HPMC Phthalate | 1:3 | 26.33±3.5 | - |
| 6 | B6 | HPMC Phthalate | 1:5 | 38.81±2.8 | 66.66±3.2 |
| 7 | B7 | Eudragit L-100-55 | 1:3 | 42.21±1.6 | - |
| 8 | B8 | Eudragit L-100-55 | 1:5 | 65.21± 2.9 | 51.55±2.3 |
| 9 | B9 | Eudragit L-100 | 1:3 | 38.95±3.2 | - |
| 10 | B10 | Eudragit L-100 | 1:5 | 63.91±3.5 | 39.55±2.1 |
| 11 | B11 | Eudragit S-100 | 1:3 | 41.10±2.8 | - |
| 12 | B12 | Eudragit S-100 | 1:5 | 69.11±3.3 | 20.55±1.9 |
| | | Different levels of polymers | | | |
| 13 | B13 | Eudragit S-100 | 1:6 | 70.12±2.9 | 21.33±1.2 |
| 14 | B14 | Eudragit S-100 | 1:8 | 56.09±1.6 | 41.55±3.5 |
| | | Incorporation of plasticizer | | | |
| 15 | B15 | TEC 5% of dry polymer weight | 1:4.75:0.25 | 54.57±2.2 | 64.41±2.1 |
| 16 | B16 | TEC 10% of dry polymer weight | 1:4.5:0.5 | 58.04±2.2 | 69.51±1.3 |
| | | Polymeric combinations | | | |
| 17 | B17 | Eudragit S100: Sodium alginate | 1:4:1 | 53.83±2.9 | 48.39±2.2 |
| 18 | B18 | Eudragit S100: Glyceryl benehate | 1:4:1 | 58.91±3.2 | 24.73±2.1 |
| | | Change of alkalizing agent | | | |
| 19 | B19 | Sodium carbonate | 1:5 | 44.92±2.1 | 48.90±1.9 |

*EE-Entrapment Efficiency
# GR-Gastric Resistance

Enteric polymers exhibit very low solubility in acid and water due to their acidic nature. One of the approaches is to utilize alkaline solutions to render it soluble and acquiescent to spray drying. Thus we have employed NaOH to solubilize enteric polymer for preparation of microparticles unless otherwise specified [16]. Some preliminary trials were undertaken for selecting basic spray drying conditions for preparation of microparticles. Preliminary trials involved incorporation of three types of enteric polymers; HPMCAS, HPMC Phthalate and Eudragit. For HPMCAS two grades; LF and HF, for HPMC Phthalate one grade and for Eudragit three grades; L-100-55, L-100 and S-100 were investigated. The batch which showed higher entrapment efficiency (respective polymer grade) underwent for gastric resistance testing. The results are displayed in Table 9. The results revealed clear dominance of

Eudragit over other enteric polymers. All the three Eudragit grades at higher drug : polymer ratio (1:5) showed higher entrapment efficiencies than other enteric polymers. Surprisingly, findings reveal no significant difference in entrapment efficiency amongst various grades of Eudragit but significant difference was found in case of gastric resistance. The reason for Eudragit S 100 to provide greater gastric resistance is due to higher pH threshold of the polymer and its polymeric backbone as compared to Eudragit L100 and Eudragit L100-55. Hence, from first part of preliminary trials batch B12 having Eudragit S 100 was found to be optimum.

In the next step of formulation development, higher levels of Eudragit S 100 were explored viz. 1:6 (B13) and 1:8 (B14) to investigate its effect on entrapment efficiency and gastric resistance. The results for the same are depicted in Table 9. The results revealed no statistical significance difference ($p>0.5$) between drug: polymer ratio; 1:5 and 1: 6 but significance difference between 1:5 and 1:8 ratio ($p<0.5$).

In the next step, plasticizer Triethyl citrate (TEC) was incorporated at 5% and 10% level of the dry polymer. Results are depicted in Table 9. Results revealed that not only entrapment efficiency was lowered but gastric resistance was significantly lowered when compared to polymer alone. The reason may be that incorporation of the plasticizer lowered the glass transition temperature (Tg) of the polymer and simultaneously increased the permeability of the microparticles membrane resulting in more ingress of the acid inside the microparticles and augmented drug release in acidic media.

Several combinations of Eudragit S-100 with either gastric insoluble polymers or polymers that swells/insoluble in gastric acid were examined. For batch containing glyceryl behenate (B18); procedure involved priorly solublizing it in part quantity of hot isopropyl alcohol and then adding into neutralized solution of Eudragit S 100. Results disclose that entrapment efficiency was lowered for both sodium alginate (B17) and glyceryl benehate (B18) but gastric resistance was diminished prominently for sodium alginate than for glyceryl benehate (Table 9). Penultimately neither of the polymeric combination was successful in enhancing gastric resistance than polymer alone. On looking deeply inside, this may be due to improper polymer-polymer miscibility resulting in no further improvement in strength of microparticle membrane. Another anticipation was made for glyceryl benehate that it would prolong the drug release in phosphate buffer pH 7.4 but on the contrary complete release was obtained in phosphate buffer pH 7.4. The reason was that major portion was Eudragit

S-100 which completely dissolved in buffer due to its pH threshold eventually responsible for complete drug release and subduing the effect of glyceryl benehate.

Lastly, alkalizing agent NaOH was majorly replaced with sodium carbonate to investigate its effect on entrapment efficiency and gastric resistance. Sodium carbonate was added into ratio of 5:1 for Eudragit S 100: Sodium carbonate and final pH was adjusted by adding NaOH to obtain pH of 9. The results are shown in Table 9. Results revealed not only diminish gastric resistance but also reduce entrapment efficiency suggesting inefficiency of sodium carbonate against NaOH as alkalizing substance.

Thus, from the preliminary trials, it revealed batch B12 containing Eudragit S 100 alone as enteric polymer gave highest gastric resistance and entrapment efficiency. In further study, various process parameters were optimized to examine their consequences on desired quality traits.

### 6.4.2. Process optimization for spray drying process

Spray drying has variegated parameters which need to be optimized to ascertain desired quality traits. The consequences of diverse process parameter on product attributes together with the range of their variation are highlighted in Table 10. Each parameter was varied at a time while keeping others constant, considering their relative impact on product attributes. The value selected for parameter investigated was carried forward in subsequent trials.

**Table 10: Different levels of process parameters that were varied during spray drying.**

| Parameters | Range of Variations | Possible effect on product attributes |
|---|---|---|
| Inlet air Temperature | 130$^{o}$C, 150$^{o}$C and 170$^{0}$C | Drying, Particle size, entrapment efficiency |
| Atomizing air pressure | 1, 2 and 3 Kg/cm$^{2}$ | Drying, particle size, gastric resistance |
| Feed solution concentration | 1.5%, 3% and 6%w/v | Drying (liquid-air ratio), particle size, gastric resistance |
| Feed solution spray rate | 1.5, 3 and 6 ml/min | Drying, Particle size |
| Aspirator volume | 30, 60 and 90% of instrument setting. | Drying; product yield |

### 6.4.2.1. Inlet air temperature

Inlet temperature was varied at three levels 130°C, 150°C and 170°C in the presence of vacuum. The feed solution concentration was 6% w/v, feed spray rate 3 ml/min, air pressure 2 kg/cms$^2$ and aspirator set volume 30%. The inlet air temperature of 130°C resulted in improper drying leading to maximum deposition of solids on the drying chamber wall instead of accumulating more into collection vessel. The resultant losss on drying (LOD) (6.98%) was also higher suggesting insufficient drying. When inlet temperature was raised to 170°C resulted in deposition of solids around mouth of the nozzle with sometimes creating blockage of nozzle, ultimately creating problems in spray drying. The resultant LOD (1.15%) was relatively satisfactory but entrapment efficiency was found to be low suggesting possible degradation of drug due to such a high temperature (Table 11). Inlet temperature of 150°C provided satisfactory drying together with maximum collection in the collector. The LOD (2.12%) was found to be satisfactory and entrapment efficiency was also found to be highest. Gastric resistance was not that much affected as that of entrapment efficiency on change of inlet temperature (Table 11). Hence, 150°C inlet air temperature was found to be optimized and was fixed for further experimental trials.

**Table 11: Results of process parameter optimization during spray drying.**

| Sr.No. | Process Parameter | Variation | EE* | GR# | Comments |
|---|---|---|---|---|---|
| P1 | Inlet Temperature | 130°C | - | - | Insufficient drying, high LOD, lesser yield |
| P2 | | 150°C | 70.91±2.3 | 19.28±1.8 | Optimum |
| P3 | | 170°C | 60.11±3.8 | 22.32±1.2 | Low entrapment efficiency, blockade of nozzle sometimes, lesser yield |
| P4 | Atomizing Air Pressure | 1 Kg/cm$^2$ | 69.28±2.3 | 17.85±1.9 | Higher particle size, difficult to maintain low pressure for operation |
| P5 | | 2 Kg/cm$^2$ | 70.12±2.9 | 21.33±1.2 | Optimum |
| P6 | | 3 Kg/cm$^2$ | 68.18±2.1 | 30.53±2.2 | Finer particle size, lower gastric resistance, lesser yield |
| P7 | Feed Solution Concentration | 1.5 % w/v | 64.57±2.2 | 35.41±2.1 | Finer particle size, lower gastric resistance |
| P8 | | 3% w/v | 69.04±2.2 | 26.81±3.3 | Finer particle size, lower gastric resistance |
| P9 | | 6% w/v | 71.06±2.9 | 19.82±2.9 | Optimum |
| P10 | Spray Rate | 1.5 ml/min | 68.15±1.9 | 20.51±2.9 | No major effect on physical attributes |
| P11 | | 3 ml/min | 70.55±1.3 | 21.82±2.3 | Optimum |
| P12 | | 6ml/min | - | - | Improper drying due to high liquid - air ratio |
| P13 | Aspirator Volume | 30% | 68.92±2.3 | 19.32±1.6 | No major effect on physical attributes, less yield |
| P14 | | 60% | 70.10±1.9 | 21.83±1.2 | No major effect on physical attributes, less yield |
| P15 | | 90% | 70.33±1.5 | 20.55±1.9 | Optimum-No major effect on physical attributes, highest yield |

*EE-Entrapment Efficiency
#GR-Gastric Resistance

### 6.4.2.2. Atomizing air pressure

Air pressure was varied at 1, 2, and 3 kg/cm$^2$, with inlet air temperature of 150°C, and all other parameters as previously mentioned. A high pressure resulted in fine particles of size (0.5 – 1.8µm). It did not affect entrapment efficiency but rather gastric resistance was found to be lower (Table 11). Also, proportion of product deposited into the scrubber was higher than into the collection vessel. The reason for lower gastric resistance may be the higher surface area provided by finer size which allowed more acidic media to diffuse in the microparticles resulting in lower gastric resistance. Thus, the results were contrary to the ideal characteristics of microparticles. The lower air pressure of 1 kg/cm$^2$ resulted in relatively larger size particles of (9 – 12) µm with higher gastric resistance (Table 11) but maintenance of

such a low pressure was difficult due to technical limitations. The air pressure of 2 $kg/cm^2$ provided particle size of around (4 – 7µm) with higher gastric resistance with no problem in machine operation (Table 11). Regardless of the air pressure, cohesive powder was obtained with poor flow properties at all the particle size ranges. The atomizing air pressure was kept at 2 $kg/cm^2$ for further experimentation.

**6.4.2.3. Feed solution concentration**

The feed solution concentration was varied at three levels 1.5%, 3% and 6% w/v. Lower concentration resulted in finer particles (0.6-1.2 µm) which may be due to slower evaporation of solvent leading to slower formation of solid wall of microparticles. Additionally, as discussed earlier gastric resistance was found to be less and more deposition of solids into scrubber due to fine particle size. On increasing feed concentration to 3%w/v improved gastric resistance. On further increasing feed solution concentration to 6%, the particle size (4 - 7 µm) simultaneously increased and provided higher gastric resistance. This may be due faster drying of particles with higher solid content. The higher solid concentration leads to formation of crust of solid faster on solvent evaporation as compare to lower solid concentration. Entrapment efficiency was not affected by feed solution concentration (Table 11). Thus, the feed solution concentration was kept as maximum level 6% w/v for further experimentation. Moreover, higher solid content permits saving of vulnerable, time, energy and solvent.

**6.4.2.4. Feed solution spray rate**

The spray rate was varied at 1.5, 3.0, and 6 ml/min, with other parameters as optimized previously and aspirator setting at 30%. The higher spray rate of 6 ml/min resulted in insufficient solvent evaporation due to high liquid- air ratio. This lead to deposition of spray mist on the wall of drying chamber and minimal deposition of solid into collection vessel. On the contrary lower spray rate of 3 ml/min and 1.5 ml/min resulted in maximum deposition of solids into the collector vessel with minimal differences in its physical properties and gastric resistance. Thus spray rate of 3ml/min was fixed due to lower time consumption than 1.5ml/min with desired product attributes.

### 6.4.2.5. Aspirator volume

The aspirator settings were kept as 30%, 60% and 90% of the instrument settings considering the lower, middle and maximum instrument settings range for continuous operation. The results revealed that higher the aspirator settings, the higher were the product recovery. The yield proportionately increased with the aspirator volume. It did not impact other product physical attributes and gastric resistance. Hence, the aspirator setting was fixed at 90% of the instrument setting.

### 6.4.3. *In vitro* drug release

*In vitro* drug release of the drug remaining stable after exposing to acidic media was carried out in 900 ml phosphate buffer pH 7.4. All the batches showed complete drug release of more than 85% in the medium selected. The *in vitro* drug release of the optimized batch B12 with process parameters as optimized above is highlighted in Fig. 7. The results reveal more than 85% drug release from formulation with low standard deviation amongst different units while incomplete release was observed from plain drug. Thus, formulation diminishes not only the variability reasons due to its solubility but also increases the solubility of the drug due to its amorphous nature.

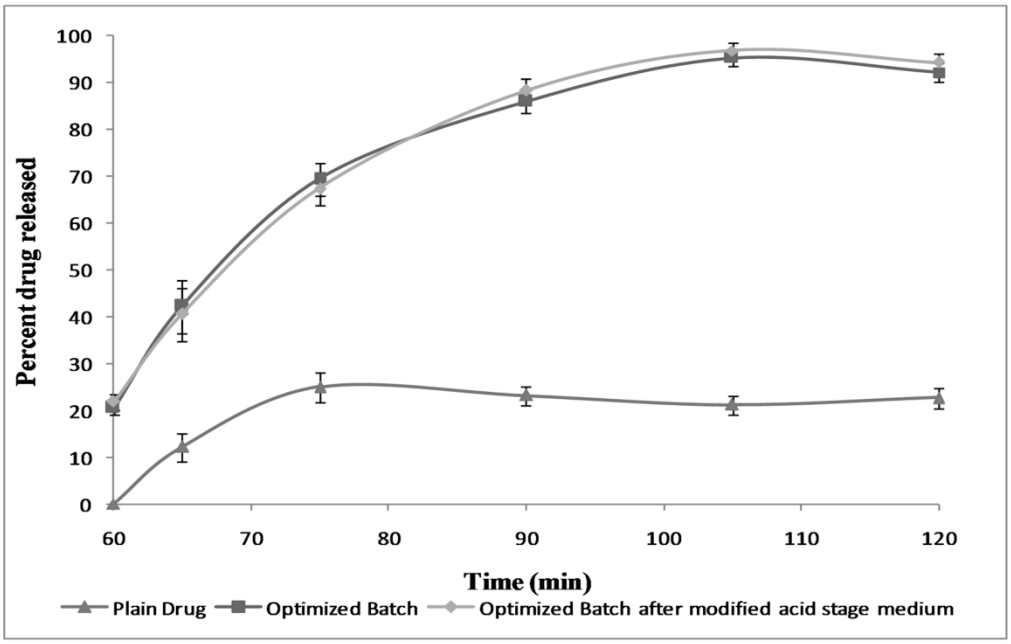


**Fig.7: Dissolution profile in 900ml, USP apparatus-II, 75 rpm, phosphate buffer pH 7.4.**

### 6.4.4. Gastric resistance and *in vitro* drug release in modified acid stage medium pH 4.5

As discussed earlier, *in vivo* pH of patients on multiple dose regimens of PPI is >4, thus microparticles of optimized batch B12 were tested in the modified acid stage medium of pH 4.5 which better simulates the gastric environment. Gastric resistance in pH 4.5 acetate buffer was found to be 21.82±1.6 which was not significantly different from gastric resistance in 0.1 N HCl. The *in vitro* drug release in phosphate buffer pH 7.4 is depicted in Fig.7. From Fig. 7, it can be observed that more than 85% of the drug released in pH 7.4 phosphate buffer media.

### 6.4.5. Characterization of microparticles

#### 6.4.5.1. DSC study

DSC spectra of LSP, physical mixture of drug and polymer, blank microparticles and drug loaded microparticles are depicted in Fig 8. DSC analysis of LSP exhibited two different events; endothermic peak at 177.41°C corresponding to melting point of the drug which was immediately followed by exothermic peak corresponding to the degradation of the drug. Physical mixtures of the drug and polymer sample showed endotherm at 70.20°C correlating to the polymer and the other one at 178.32°C correlating to the LSP. Moreover exothermic peak correlating to degradation of LSP was also observed. In case of microparticles, complete absence of endothermic as well as exothermic peak of LSP was depicted signifying drug is molecularly dispersed within the polymer, stabilizing effect on drug and restraining its degradation. The thermal behavior of drug loaded microparticles was similar to the blank micorparticles, thus supporting the above hypothesis.

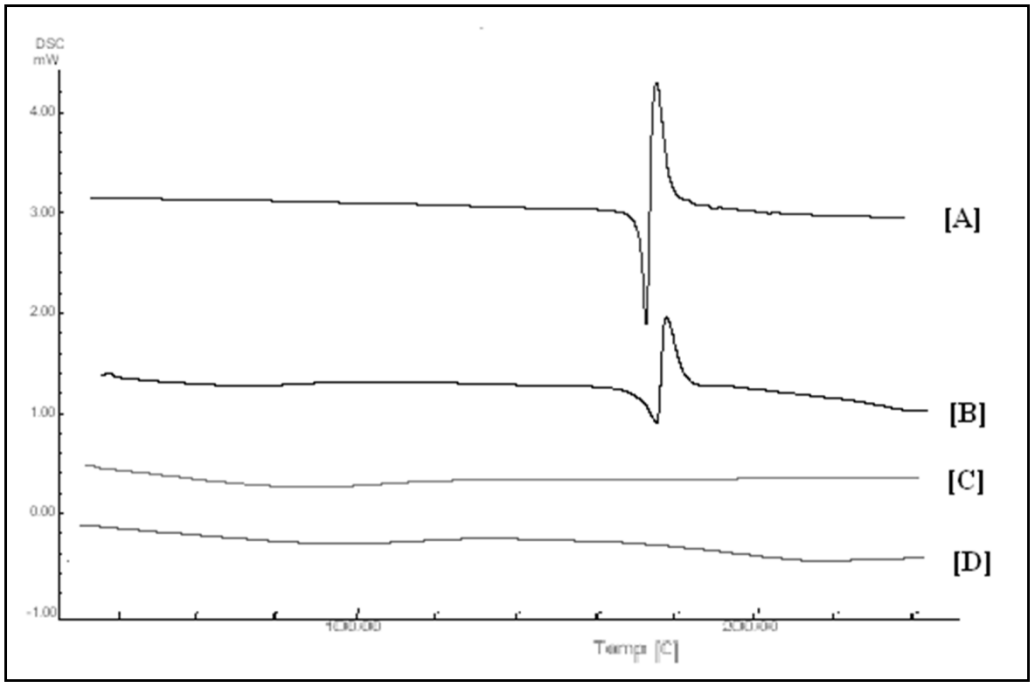


**Fig. 8: DSC spectra for [A] LSP, [B] Physical mixture, [C] Blank microparticles and [D] drug loaded microparticles.**

### 6.4.5.2. FT-IR study

During preparation of microparticles, there are chances of interaction between the drug and the polymer. As we know enteric Eudragit polymers contain acidic functional groups and if they interact with the drug can lead to degradation of it. To investigate any lack of interaction between drug and polymer, FT-IR spectroscopy was used. The FT-IR spectra of drug, physical mixture, blank microparticles and drug loaded microparticles are displayed in Fig 9. The FT-IR spectra of LSP exhibited characteristics peaks at 3238, 2983, 1581, 1476, 1283 and 1117, signifying stretching vibrations of –NH, $–CH_2$-, aromatic ring, –NH bending, C-N of pyridyl ring and the ether bond respectively [17]. The polymer sample exhibited the C=O vibrations of the carboxylic acid groups at 1705 $cm^{-1}$ and at 1730 $cm^{-1}$ for esterified carboxylic acid group. When polymer was neutralized with NaOH its ionization occurred and the characteristic peak of carboxylic acid group at 1705 $cm^{-1}$ was replaced by band at 1560 $cm^{-1}$ corresponding to the anti- symmetrical vibration of the $–COO^-$ [16]. These changes were seen in both blank and drug loaded microparticles. The esterified carboxylic acid peak remained at the same position at 1730 $cm^{-1}$ signifying that it did not involve in any type of interaction. Now, the FT-IR spectra of the drug loaded

microparticles was compared with the FT-IR spectra of physical mixture and plain drug. The spectra did not show any shift in its characteristic peaks of LSP in microparticles suggesting no new chemical bond formation. Thus, this observation ruled out the possibility of interaction between drug and polymer indicating that the LSP was physically dispersed in the Eudragit S-100.

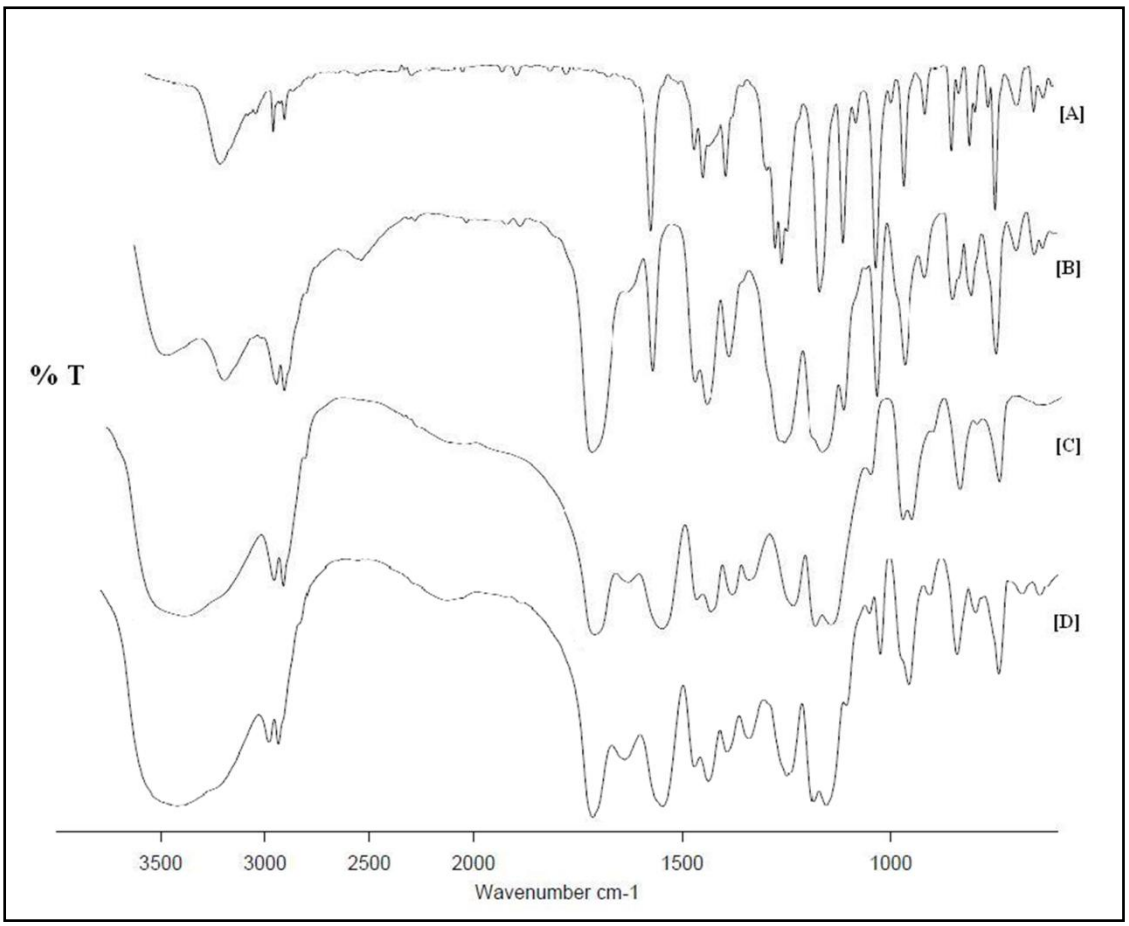


**Fig. 9: FT-IR spectra for [A] LSP, [B] Physical mixture, [C] Blank microparticles and [D] drug loaded microparticles.**

### 6.4.5.3. PXRD Study

PXRD diffractograms of pure LSP, physical mixture, blank microparticles and drug loaded microparticles are depicted in Fig. 10. The variegated distinct peaks appearing in the diffractogram discloses that LSP is in crystalline form with charaecteristic peaks at an angle of 2θ at 11.40, 12.76, 14.24, 16.90, 17.50, 18.62, 22.29, 24.90 and 27.73. Blank microparticles were characterized by halo pattern or complete absence of any peaks in diffractogram. The XRD peaks of the LSP were found in the same position in physical mixture while complete absence was seen in the drug loaded

microparticles indicating amorphization of the drug. The results were in line with the DSC data confirming amorphization of the drug in the microparticles.

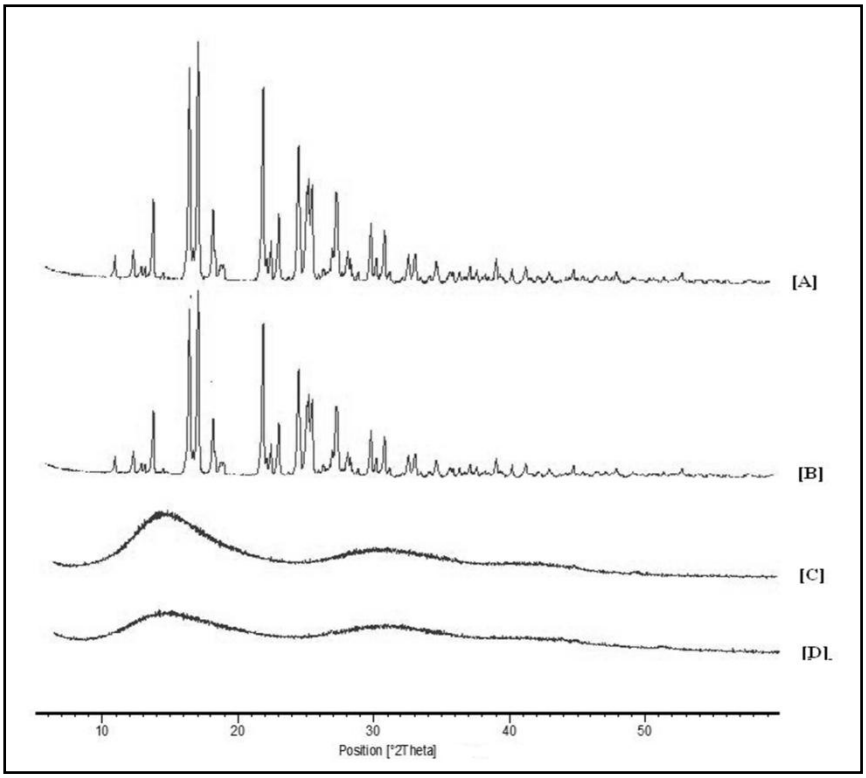


**Fig. 10: PXRD spectra for [A] LSP, [B] Physical mixture, [C] Blank microparticles and [D] drug loaded microparticles.**

### 6.4.5.4. SEM study and powder characteristics

The results of the SEM analysis for various batches are demonstrated in Fig. 11. The results disclose that microparticles represented spherical and smooth surface. The powder characteristics of the optimized batch B12 is depicted in Table 12. From the Table 12, results revealed that microparticles had poor flow according to Carrs's and Hausner's ratio comparison. Moreover, bulk density was found to be higher as small particles are usually denser and exhibit higher bulk density. Additionally, irrespective of process conditions, all the batches exhibited poor flow characteristics of powder.

**Table 12: Powder characteristics of microparticles for optimized batch**

| Batch No. | Bulk density | Tapped density | Compressibility Index | Hausner Ratio |
|---|---|---|---|---|
| B12 | 0.20 | 0.33 | 0.3939 | 1.65 |

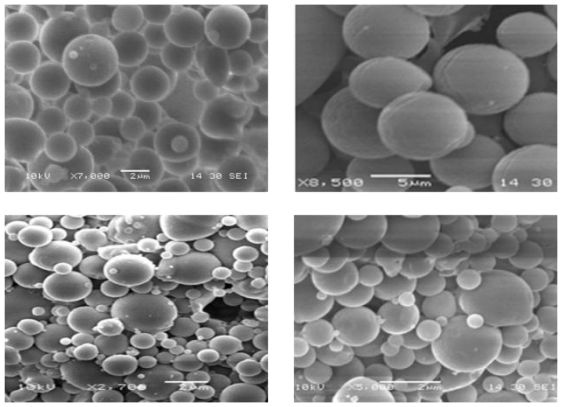

**Fig. 11: Topographical images of microparticles carried out by SEM.**

### 6.4.6. Product Suitability

In the research envisaged, enteric microparticles were prepared in single step by spray drying technology. Employing this technique facilitate formulation development in ready to formulate form. The microparticles resulted in significant enhancement of gastric resistance (Table 9) together with improved solubility in the dissolution medium (Fig. 7). The microparticles were directly blended with fillers (Microcrystalline cellulose; Avicel PH 102 and lactose monohydrate (Pharmatose DCl 11), superdisintegrant (crospovidone) glidant (talc) and lubricant (magnesium stearate) and filled directly into hard gelatin capsule of size 0 at fill weight of 400 mg. Thus, it reduces overall processing time and augments formulation productivity.

### 6.4.7. Batch reproducibility and stability studies

The three batches of optimized formulation B12 were prepared and evaluated for physicochemical properties under identical experimental conditions. The entrapment efficiency, gastric resistance and *in vitro* drug release did not show significant difference between within three set of batches revealing reliability and reproducibility of manufacturing process.

At all the sampling time in stability studies including on completion of stability studies, microparticles demonstrated shape and powder characteristics similar to those of initial samples. The results of the stability data are displayed in Table 13. The result demonstrated no significant change in entrapment efficiency and gastric resistance for initial, long term and accelerated stability sample. The similarity factor (f2) [18] was employed for comparison of dissolution profiles on each time point. It

ranged from 76 to 85. Thus it showed comparable dissolution profile with initial samples.

**Table 13: Stability study data for optimized batch**

| Batch No. | Entrapment Efficiency | | | Gastric Resistance | | |
|---|---|---|---|---|---|---|
| | Initial | 3 months 25±2 ◦C/60 ± 5% RH | 3months 40±2 ◦C/75± 5% RH | Initial | 3 months 25±2 ◦C/60± 5% RH | 3months 40±2◦C/75± 5% RH |
| B12/microparticles | 69.11±3.32 | 69.23±2.89 | 67.20±1.92 | 20.55±1.9 | 21.39±1.2 | 21.98±1.5 |
| B12/capsule formulation | 69.11±3.32 | 68.12±2.23 | 66.85±2.81 | 20.55±1.9 | 20.92±1.1 | 22.11±1.2 |

## 6.5. Conclusion

With the mounting awareness of spray drying techniques for preparation of drug microparticles commercially, the usefulness of it has now prudently entered in the realm of research and industry for understanding of process or formulation variable rationally. The manuscript describes development and optimization of enteric microparticles of LSP using spray drying. In an endeavor to accomplish the objectives preliminary trials were undertaken to screen type of enteric polymer and its levels. The Eudragit S100 was found to be the optimized polymer at drug:polymer ratio 1:5 with gastric resistance of around 20% and more than 85% drug release in phosphate buffer pH 7.4. The gastric resistance was not affected by modified acid stage medium of pH 4.5 acetate buffer. Finally, the process parameters were optimized to get reproducible results. The optimized process comprised of inlet temperature of 150°C, atomizing air pressure of 2 kg/cms$^2$, feed solution concentration of 6%w/w, feed solution spray rate of 5ml/min, and aspirator volume of 90%. Microparticles by SEM revealed smooth surface and spherical morphology. DSC, PXRD and FT-IR confirmed that LSP was physically dispersed in the polymer. The product was found to be stable on 3 months accelerated and long term condition as per ICH Q1A(R2) guidelines.

Hence, the developed microparticles of LSP can provide prudently a better approach for its enteric delivery in terms of formulation aspect that can be directly filled into capsule with nominal usage of excipients. Moreover, the manufacturing method employed can be easily adopted in industries.

## 6.6. References


1. Barradell, L.B., Faulds, D., McTavish D., 1992. Lansoprazole, a review of its pharmacodynamic and pharmacokinetic properties and its therapeutic efficacy in acid-related disorders. Drugs 44, 225–250.
2. Wua, C., Suna, L., Suna, J., Yang, Y., Renb, C., Ai, X., Lianb, H., He, Z., 2013. Profiling biopharmaceutical deciding properties of absorption of lansoprazole enteric-coated tablets using gastrointestinal simulation technology. Int. J. Pharm. 453, 300–306.
3. Horn, JR., Howden, C.W., 2005. Review article: similarities and differences among delayed release proton-pump inhibitor formulations. Aliment. Pharmacol. Ther. 22, 20–24.
4. Budavari S., 1996. 12th edn., The Merck Index, ed., Merck and Co., Inc., Rahway, NJ, p. 916.
5. Reynold J.E.F., 1999, 32nd edn., Martindale, The Extra Pharmacopeia, ed., Royal Pharmaceutical Society, London, p. 1196.
6. Al-Zehouri, J., El-Subbagh, H.I., Al-Badr, A.A., 2001. Lansoprazole. In: Florey, K. (Ed.), Analytical Profiles of Drug Substances. Academic Press, New York. 28, 117-151.
7. Lansoprazole-Pubchem. Available at http://pubchem.ncbi.nlm.nih.gov/compound/ lansoprazole #section=Top
8. Lansoprazole-Dailymed. Available at http://dailymed.nlm.nih.gov/dailymed/drug Info.cfm? setid =bf170659-a4f3-4ff7-8a0f-b3a0a2d02ff5
9. Kubo, K., Oda, K., Kaneko, T., Satoh, H., Nohara, A., 1990. Synthesis of 2-[[(4-fluoroalkoxy-2-pyridyl)methyl]sulfinyl]-1H- benzimidazoles as antiulcer agents. Chem. Pharm. Bull. 38, 2853-8.
10. Gremse, D.A., 2001. Lansoprazole: Pharmacokinetics, pharmacodynamics and clinical uses. Exp. Opin. Pharmacother. 2,1663-1670.
11. ICH harmonised tripartite guideline, November 2005. Validation of analytical procedures: text and methodology. Q2 (R1).
12. Tabatar, T., Makino, T., Kashihara, T., Hirai, S., Kitamori, N., Toguchi, H., 1992. Stabilization of a new antiulcer drug (Lansoprazole) in the solid dosage forms. Drug Dev. Ind. Pharm. 18, 1437–1447.

13. Monographs, Medicinal and Pharmaceutical substances, Lansoprazole delayed release capsule, United States Pharmacopoeia. 2006**.**
14. Rohss, K., Lind, T., Wilder-Smith, C., 2004. Esomeprazole 40 mg provides more effective intragastric acid control than lansoprazole 30 mg, omeprazole 20 mg, pantorpazole 40 mg and rabeprazole 20 mg in patients with gastro-oesophageal reflux symptoms. Phamacodynamics. 60, 531–539.
15. ICH harmonised tripartite guideline, February 2003. Stability testing of new drug substances and products Q1A(R2).
16. Cilurzo, F., Minghetti, P., Selmin, F., Casiraghi, A., Montanari, L., 2003. Polymethacrylate salts as new low-swellable mucoadhesive materials. J. Control. Reles. 88, 43–53.
17. Zhang, X., Sun, N., Wu, B., Lu, Y., Guan, T., Wu, W., 2008. Physical characterization of lansoprazole/PVP solid dispersion prepared by fluid-bed coating technique. Powder Tech. 182, 480–485.
18. Costa P, Sousa Lobo JM (2001) Modeling and comparison of dissolution profiles. Eur J Pharm Sci 13:123–133.